

Transport and elastic scattering times as probes of the nature of impurity scattering in single and bilayer graphene.

M. Monteverde, C. Ojeda-Aristizabal, R. Weil, M. Ferrier, S. Guéron, H. Bouchiat, and J.N. Fuchs
LPS, Univ. Paris-Sud, CNRS, UMR 8502, F-91405 Orsay Cedex, France

D. Maslov
*LPS, Univ. Paris-Sud, CNRS, UMR 8502, F-91405 Orsay Cedex,
France and University of Florida Gainesville, FL 32611, USA*

Both transport τ_{tr} and elastic scattering times τ_e are experimentally determined from the carrier density dependence of the magnetoconductance of monolayer and bilayer graphene. Both times and their dependences in carrier density are found to be very different in the monolayer and the bilayer. However their ratio τ_{tr}/τ_e is found to be of the order of 1.5 in both systems and independent of the carrier density. These measurements give insight on the nature (neutral or charged) and spatial extent of the scattering centers. Comparison with theoretical predictions yields that the main scattering mechanism in our graphene samples could be due to strong scatterers of short range, inducing resonant scattering, a likely candidate being vacancies.

PACS numbers: 63.22.Np, 73.23.Hk, 73.21.Ac

Since the discovery of the fascinating electronic properties of graphene [1] due to its electronic spectrum with linear dispersion and a perfect electron-hole symmetry at the Fermi level [2], the nature of scattering impurities as well as the amplitude of electron-electron interactions have been shown to play an essential role in determining the carrier density dependence of the conductance as well as the formation of Landau levels at high magnetic field. The wave vector and energy dependences of the impurity potential are known to determine the characteristic scattering times of the charge carriers. It is important to distinguish the transport time τ_{tr} , which appears in the Drude conductivity as the relaxation of the current operator, from the elastic scattering time τ_e which is the life time of a plane wave state [3]. Their calculation involve different angular integrals of the cross section of the scattering amplitude. This leads to different values for τ_{tr} and τ_e as soon as the Fourier components of potential depend on wavevector q . A large ratio τ_{tr}/τ_e indicates that forward scattering is favored over lateral scattering so that the transport is not perturbed much by this type of scattering. Such a case is observed in 2D electron gases (2DeG) confined in GaAs/GaAlAs heterojunctions where the scattering potential is produced by the remote charged Si donors far from the 2DeG [4].

The nature of the main scattering mechanism limiting the carrier mobility in graphene is still subject to controversy. It has indeed been shown [5] that a "white noise" q independent scattering potential produced by neutral localised impurities leads to a conductivity independent of the carrier density n_c , in contradiction with experimental results where a linear increase with n_c of the conductance is generally observed. Scattering on charged impurities has also been considered [6]. It originates from a q dependent Coulomb potential whose carrier density dependence can be obtained in the Thomas Fermi ap-

proximation. This leads to a linear n_c -dependence of the conductivity both for the monolayer and the bilayer in the range of densities where the dispersion relation of electrons and holes can be described by a constant effective mass. Recent experiments were performed in order to check this hypothesis by measuring the modification of the gate dependent conductivity when immersing graphene samples in high dielectric media. The conclusions of these experiments are controversial [7, 8] and do not clearly point to the nature of the scattering mechanism. Alternative explanations have been proposed involving resonant scattering centers with a large energy mismatch with the Fermi energy of carriers [9].

In order to get more insight on the scattering mechanism in graphene, we have determined both τ_e and τ_{tr} by investigating the magnetotransport in monolayer and bilayer exfoliated graphene samples. At high magnetic field, when the cyclotron frequency is larger than the inverse elastic scattering time, the magneto-conductivity exhibits Shubnikov de Haas (SdH) oscillations related to the formation of Landau levels. The broadening of these levels at low temperature yields τ_e , while the low field quadratic magneto-conductivity yields τ_{tr} independently of any assumption on the gate voltage dependence of the carrier density yielding misleading results in inhomogeneous samples [8].

The samples were fabricated by exfoliation of natural graphite flakes and deposition on a doped silicon substrate with a 285 nm thick oxide which allows its visual detection using an optical microscope. The carrier density can be tuned from electrons to holes through the charge neutrality point by applying a voltage on the doped silicon backgate. The single and bilayer samples were identified using Raman spectroscopy. The electrodes were fabricated by electron beam lithography and sputter deposition of 40 nm thick palladium. In the fol-

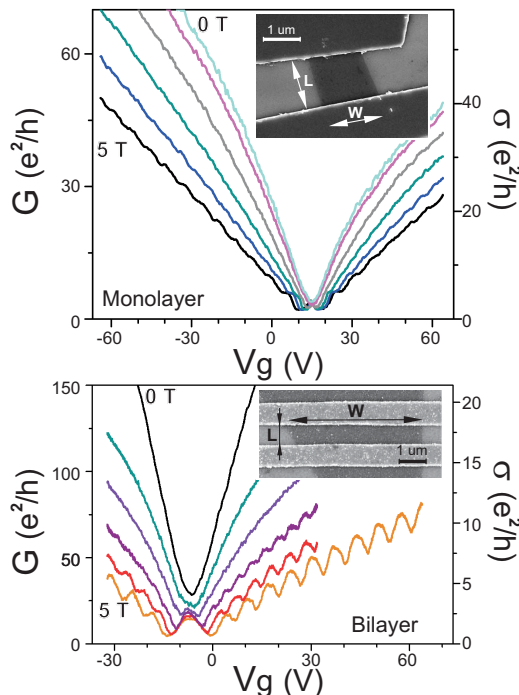


FIG. 1: Gate voltage dependence of the conductance measured for several values of magnetic field spaced by 1 T. The contact resistances have been subtracted. Top panel: monolayer. Bottom panel: bilayer. The insets are electron micrographs of the measured samples.

lowing we discuss data obtained on 2 samples, a monolayer and a bilayer of respective dimensions $W = 1.6\mu\text{m}$, $L = 1.3\mu\text{m}$ and $W = 4.8\mu\text{m}$, $L = 0.7\mu\text{m}$. L is the distance between the voltage probes covering nearly the whole sample width W (see micrographs on Fig.1). The contribution of both contact resistances were measured to be equal to $20\ \Omega$ for the bilayer and estimated to be $200\ \Omega$ for the monolayer and systematically subtracted from the data. The gate voltage dependence of the conductance is shown for both samples in different magnetic fields in Fig.1. At zero magnetic field one observes a linear increase of the conductance on both sides of its minimum at the neutrality point for the bilayer whereas this dependence is slightly sublinear for the monolayer at low doping. Note however that the value of conductivities for both samples only differ by at most 25%. Above 2T steps occur at conductance values of the order of $(4n+1/2)e^2/h$ as expected for the monolayer. The oscillations observed on the bilayer with a maximum of conductance at the neutrality point look more unusual but can be understood taking into account the aspect ratio of the sample, as will be discussed in more detail below.

In the following we describe how we extract the char-

acteristic times τ_{tr} and τ_e from the field dependences of the conductance, (see Fig.2) for the bilayer and the monolayer. We also show why we find this method more reliable than the usual analysis of the gate voltage dependence of the conductance. At low magnetic field the transport time is deduced from the analysis of the classical quadratic magnetoresistance:

$$(R(B) - R(0))/R(0) = (\omega_c\tau_{tr})^2 = \alpha B^2 \quad (1)$$

where $\omega_c = eB/m^*$ is the cyclotron frequency and $m^* = \hbar k_F/v_F$ is the cyclotron mass. For the bilayer m^* is just the effective mass $m_{eff} = 0.035m_e$, independent of the carrier density in the range of gate voltage investigated [10]. This value of m_{eff} is confirmed from the analysis of the temperature dependence of the SdH oscillations (see below). The experimental determination of the coefficient α thus yields directly the transport time as a function of the gate voltage for the bilayer. In the monolayer, where carriers behave as massless particles of constant velocity $v_F \simeq 10^6\text{m/s}$, the analysis is not so straightforward. The cyclotron frequency now explicitly depends on the Fermi wavevector k_F which in an homogeneous sample is related to the gate voltage V_g through the carrier density n_c by:

$$k_F^2/\pi = n_c = C|V_g - V_0|/e \quad (2)$$

where C is the capacitance per unit surface between the doped silicon substrate and the graphene foil and V_0 is the gate voltage at the charge neutrality point. As already noticed in [11] this relation between the carrier density and the gate voltage is not reliable in inhomogeneous samples where regions of holes coexist with regions of electrons, as happens close to the charge neutrality point (formation of puddles). This is why we have chosen to eliminate k_F between the expressions of the Drude conductivity at zero field :

$$\sigma = 2(e^2/h)k_F v_F \tau_{tr} \quad (3)$$

and the coefficient $\alpha = [ev_F\tau_{tr}/\hbar k_F]^2$ in order to extract τ_{tr} independently of any assumption on the gate voltage dependence of n_c :

$$\tau_{tr} = \left[\frac{\pi\hbar^2\sqrt{\alpha\sigma}}{e^3v_F^2} \right]^{1/2} \quad (4)$$

This analysis gives a different and certainly more reliable determination of the transport time than the sole analysis of the zero field Drude conductivity especially near the charge neutrality point.

The elastic time is extracted from the the damping of the SdH oscillations [12] which reads after subtraction of

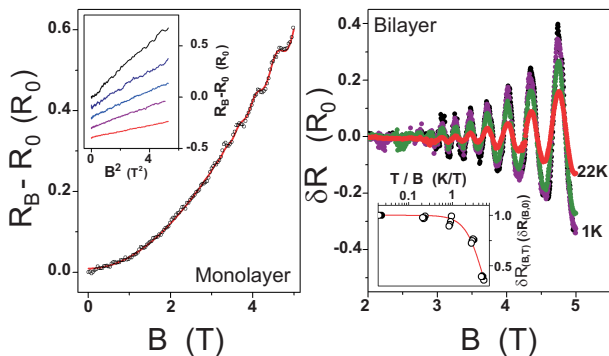


FIG. 2: Analysis of the magnetoresistance. Right panel: Bilayer sample showing $1/B$ periodic Shubnikov de Haas oscillations measured for different temperatures. The ratio τ_{tr}/τ_e is deduced from the low temperature exponential decay of these oscillations. The temperature dependence of the amplitude of the oscillations is depicted in the lower inset and fitted according to $D_T = \gamma/\sinh(\gamma)$ with $\gamma = 2\pi^2 k_B T/\hbar\omega_c$. The effective mass can be determined with this fit and is found to be $m_{eff} = 0.035 \pm 0.002 m_e$. Left panel: Analysis of the magnetoresistance of the monolayer sample in units of R_0 the resistance at zero fields. Dots: experimental points at $T = 1K$. Continuous line: fit according to expressions 1 and 5. The upper inset shows the B^2 linear dependence of the low field magnetoresistance for different gate voltages. The largest slope corresponds to the vicinity of the Dirac point. τ_{tr} is extracted from these plots. All the curves have been shifted along the Y axis for clarity purposes.

the magnetoresistance quadratic background:

$$\delta R(B)/R_0 = 4D_T \exp\left[-\frac{\pi}{\omega_c \tau_e}\right] \cos\left[\frac{\pi E_F}{\hbar\omega_c} - \phi\right] \quad (5)$$

The prefactor $D_T = \gamma/\sinh(\gamma)$ with $\gamma = 2\pi^2 k_B T/\hbar\omega_c$ describes the temperature damping of the oscillations on the scale of $\hbar\omega_c/(2\pi^2 k_B)$ neglecting the inelastic scattering contribution. This yields a determination of the effective mass for the bilayer which confirmed the expected theoretical value $2\hbar^2 t_{\perp}/(9a^2 t_{\parallel}^2)$ where t_{\parallel} , t_{\perp} are the in-plane, transverse coupling energies and a is the carbon-carbon distance [10]. The phase ϕ of the SdH oscillations depends on the aspect ratio of the sample as discussed below. The exponential decay of the $1/B$ periodic SdH oscillations is governed by $\exp(-\beta/B)$ where $\beta = \pi\hbar k_F/ev_F\tau_e$. The ratio τ_{tr}/τ_e is then directly given by $\beta\sqrt{\alpha}/\pi$. The Fermi wave vector dependences of τ_{tr} and the ratio τ_{tr}/τ_e is given in Fig.3 for both samples. The Fermi wave vector is deduced from the conductivity through $k_F = \sigma/2(e^2/h)v_F\tau_{tr}$. We observe different behaviors for the monolayer where τ_{tr} is minimum at the charge neutrality point and the bilayer where on the other hand it is maximum. In both cases, in spite of rather large variations of τ_{tr} the ratio τ_{tr}/τ_e is independent of k_F . It is equal to 1.5 ± 0.2 for the monolayer and 1.4 ± 0.1 for the bilayer in the whole range explored

which corresponds to a carrier density varying approximately between $1.5 \cdot 10^{11}$ and $5 \cdot 10^{12} cm^{-2}$. Note also that these different transport times for the bilayer and the monolayer correspond to nearly identical transport mean free path $l_{tr} = v_F\tau_{tr}$ for both samples the conductivity of which only differ by 20% in the whole range of gate voltage investigated. The maximum value of l_{tr} is about 100nm which is smaller than the length of the shortest sample indicating a regime of diffusive transport in the range of gate voltage explored. Finally it is also possible to fit the gate voltage dependences of the conductance at 5T depicted in Fig.1 using the determination of τ_e described above. The two wire magnetoconductance measured results from a mixing of the diagonal (σ_{xx}) and the non-diagonal (σ_{xy}) components of the conductivity tensor [13, 14]. The aspect ratio of the sample determines the relative weight of σ_{xx} and σ_{xy} in the SdH oscillations of $R(B)$. The phase ϕ of the oscillations is equal to 0 for long narrow samples and π for wide short samples such as the bilayer sample investigated here. For a detailed fit of the gate dependence we used the expressions derived by Abanin and Levitov [13] relating, within the semi circular model, the filling factor ν dependences of the conductivity tensor: $\delta_n\sigma_{xx}$ and $\delta_n\sigma_{xy}$ between the $n+1$ th and the n th Landau levels of filling factor ν_n (corresponding to a carrier density equal to $\nu_n B/\Phi_0$):

$$\delta_n\sigma_{xx} \sim \exp[-\lambda [(\nu - (1/2)(\nu_n + \nu_{n+1}))^2]] \quad (6)$$

$$\delta_n(\sigma_{xx})^2 + (\delta_n\sigma_{xy} - \sigma_{xy,n}^0)(\delta_n\sigma_{xy} - \sigma_{xy,n+1}^0) = 0$$

where $\sigma_{xy,n}^0$ is the quantised Hall conductivity at the n th plateau which is $4(n+1/2)e^2/h$ and $4ne^2/h$ for the mono and the bilayer respectively. The parameter $\lambda = 4 \ln 2/\Gamma_\nu^2$ is related to $1/\tau_e$ via the disorder broadening of the Landau levels $\Gamma_E = \hbar\sqrt{2\omega_c/\pi\tau_e}$ [15] through the relations:

$$\Gamma_\nu = \Gamma_E \frac{2}{\hbar v_F} \sqrt{\frac{\nu_n \Phi_0}{\pi B}}, \quad \lambda = \ln 2 \frac{\pi^2 v_F^2 \tau_e B}{2\omega_c \nu_n \Phi_0} \quad (7)$$

A good agreement between the experimental data and the 2 wires gate dependent conductance of the monolayer calculated from the conductivity tensor [13, 14] is obtained taking the filling factor dependence of λ of eq. 7 see Fig.4. Concerning the bilayer which is much shorter, we had to modify the semi-circular relation in a similar way as done in ref[14]. These last results constitute an independent check of the validity of our approach.

We now compare our results on τ_e and τ_{tr} to recent theoretical predictions. We first consider scattering on charged impurities which has given rise to intensive theoretical investigations [5, 6]. In particular the question of the difference between τ_e and τ_{tr} has been addressed for a graphene monolayer [16]. Our findings are qualitatively compatible with the predictions corresponding to strongly screened charged impurities characterized by the

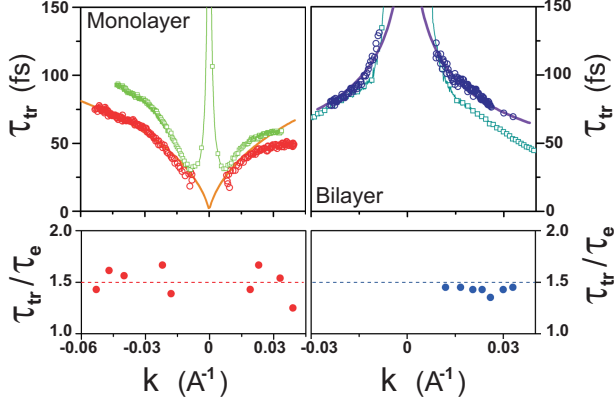


FIG. 3: Fermi wavevector dependence of τ_{tr} extracted from the B^2 dependence of the low field quadratic magnetoresistance according to expression 4 (dark circles) in comparison with the value τ_{tr} extracted from the sole zero field Drude conductivity (light squares). The continuous lines are the fits according to the resonant impurity model see eq.8. Left panel: monolayer. Right panel: bilayer. Lower panels: ratio τ_{tr}/τ_e deduced from the low temperature exponential decay of the SdH oscillations.

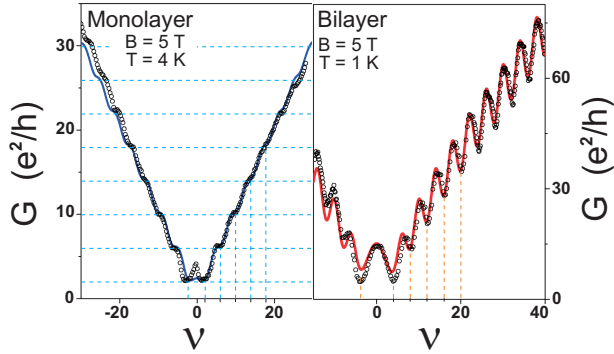


FIG. 4: Comparison of $G(\nu)$ at 5T for both samples with the expression of the conductance derived in ref.[13] corresponding to the aspect ratio L/W of each sample and using eq. 6, 7 with $\tau_e(k_F)$ determined above. The dashed vertical lines indicate the positions of ν_n which, as expected, are different for the monolayer $\nu_n = \pm 4(n + 1/2)$ and the bilayer $\nu_n = \pm 4n$. The conductance quantisation is well obeyed for the monolayer but it is not the case for the bilayer. This is well explained according to [13, 14] by the very small aspect ratio of the sample.

Thomas Fermi wave vector $q_{TF} = e^2 k_F / \epsilon \pi \hbar v_F$, where ϵ is the dielectric constant of silicon oxide. For the monolayer q_{TF}/k_F is a constant $\simeq 3$. The scattering cross section is then proportional to the Fermi wave length. Both τ_{tr} and τ_e are expected to increase linearly with density, in qualitative agreement with our results. When the impurities are located close to the graphene foil the ratio τ_{tr}/τ_e is expected to be equal to 2 and independent

of the carrier density, just like for neutral short range impurities. This factor 2 compared to the value 1 expected in standard 2D systems is due to the absence of backscattering. Since our experiments point to a ratio τ_{tr}/τ_e significantly lower than 2, it could indicate the presence of intervalley scattering due to a potential whose range is of the order of $a = 1.4\text{\AA}$. Concerning the bilayer the relation $q_{TF} = m_{eff} e^2 / \hbar^2 \pi \epsilon$ independent of the carrier concentration is predicted. This yields for the ratio q_{TF}/k_F a $1/\sqrt{n_c}$ dependence varying between 3 at high doping and 12 close to the neutrality point. The conductivity is expected to be linear in n_c with a plateau at low doping due to a residual disorder induced density [17]. However τ_{tr} is predicted to be independent of n_c which does not really agree with our data where both scattering times are found to increase at low doping. It is also not obvious whether it is reasonable to use the Thomas Fermi approximation in the bilayer system in the low carrier density limit where the screening length is notably smaller than the Fermi wave length. We also note that the predictions of [17] would yield a conductivity strongly reduced for the bilayer compared to the monolayer for the same concentration of impurities which is not the case in our experiment.

An alternative explanation could come from the presence of resonant scattering which may result from vacancies or any other kind of short range scattering of short range R with a large potential energy compared to the kinetic energy of the carriers [9]. It is characterized by a transport cross section:

$$A_{tr} \simeq \frac{\pi^2}{k_F l n^2(k_F R)} \quad (8)$$

in the limit $k_F R \ll 1$. The resulting transport time $\tau_{tr} = 1/(n_i v_F A_{tr})$ (n_i is the concentration of impurities) is thus proportional to k_F/v_F leading to a conductance increasing like n_c with logarithmic corrections both for the monolayer and the bilayer. The dependences of τ_{tr} as a function of the Fermi wave vector (see Fig.3) both for the bilayer and monolayer samples are compatible with the square logarithmic dependence of expression 8. It is even possible from these fits to estimate the range of the impurity potential $0.2 \leq R \leq 0.8\text{\AA}$ and the concentration of impurities $n_i = 8 \pm 2 \cdot 10^{11} \text{cm}^{-2}$ which are identical for both samples. This is of the order of the minimum value of the carrier density $n_{min} = 1.5 \cdot 10^{11} \text{cm}^{-2}$ we experimentally extract. It is also interesting to note that the minimum conductivity expected for this resonant impurity model: $\sigma_{min} = (2e^2/\pi h)(n_{min}/n_i) \ln^2(R\sqrt{\pi n_{min}}) = 3.7e^2/h$ and $4.5e^2/h$ for the monolayer and the bilayer respectively. These values are of the order of magnitude of the observed experimental values which are 3.3 and 4.1 e^2/h . This analysis also corroborates our results on the ratio τ_{tr}/τ_e indicating scatterers which range is of the order of a . Whereas the resonant character is not essential

for the validity of eq.8 for massive carriers (corresponding to the bilayer) [18], it has been shown that it is essential for mass-less carriers in the monolayer [19]. The resonant like character in a wide range of Fermi energy, although not straightforward, has been demonstrated in the case of scattering centers created by vacancies in graphene [20]. As shown in detail on the on-line supplementary materials it is not necessary to tune precisely k_F to observe the ln^2 dependence of expression 8. Moreover it is interesting to compare our determination of $R = 0.7\text{\AA}$ with the expected value derived in [20] which is $a/2 = 0.7\text{\AA}$. In conclusion, our results indicate that the main scattering mechanism in our graphene samples could be due to strong scatterers whose range is of the order of a inducing resonant (but not unitary) scattering; a likely candidate being vacancies as observed recently in transmission electron microscopy [21].

Aknowlegments: We thank R.Deblock, M. Goerbig, G. Montambaux and A. Kasumov for fruitful discussions. This work was supported by the EU-STREP program HYSWITCH. and the "CEE MEST CT 2004 514307 EMERGENT CONDMATPHYS Orsay" grant.

-
- [1] A. K. Geim, K. S. Novoselov, Nature Mater. 6, 183 (2007).
 - [2] P.R. Wallace, Phys.Rev **71**,622 (1947)
 - [3] Eric Akkermans and Gilles Montambaux "Mesoscopic Physics with electrons and photons".Cambdrige University Press, (2007).

- [4] P.T. Coleridge Phys. Rev. **B 44**, 3793 (1991).
- [5] N. Shon and T. Ando J. Phys. Soc. Japan **67**, 2421 (1998); T. Ando, J. Phys. Soc. Japan **75**, 074716 (2006); K. Nomura, A. H. MacDonald, Phys. Rev. Lett. **96**, 256602 (2006).
- [6] S.Adam et al. arXiv:0812.1795
- [7] T. M. Mohiuddin *et al* arXiv:0809.1162
- [8] S.Adam, S.Cho , M. Fuhrer and S. das Sarma Phys. Rev.Lett,**101** ,04604 (2008).
- [9] M. I. Katsnelson, K. S. Novoselov, Solid State Commun. **143**,3 (2007), T.Stauber, N.M.T. Peres and F.Guinea Phys.Rev.**B 76**,205423 (2007).
- [10] A. H. Castro Neto, F. Guinea, N. M. Peres, K. S. Novoselov, and A. K. Geim Rev. Mod. Phys. **81**, 109 (2009).
- [11] Sungjae Cho and Michael S. Fuhrer Phys. Rev. **B 77**, 081402 (2008).
- [12] I.M. Lifshitz and A.M. Kosevich, Zh. Eksp. Teor. Fiz. **29**, 730 (1955) [Sov. Phys. JETP 2, 636 (1956)].
- [13] D.A. Abanin and L.S. Levitov Phys.Rev.**B 78**,035416 (2008).
- [14] J.R. Williams et.al. arXiv:0810.3397
- [15] T.Ando and Y.Uemura, J.Phys. Soc.Jpn, **36**, 959 (1974).
- [16] E.H. Hwang and S.das Sarma Phys.Rev.**B 77**,195412 (2008).
- [17] Shaffique Adam and S.das Sarma Phys.Rev.**B 77**,115436 (2008).
- [18] Sadhan K. Adhikari Am.J.Phys.**54**, 362 (1986).
- [19] D.S. Novikov, Phys.Rev.**B 76**,245435 (2007).
- [20] D. Basko, Phys.Rev.**B 78**,115432 (2008).
- [21] Jannik C. Meyer, C. Kisielowski, R. Erni, Marta D. Rossell, M. F. Crommie, and A. Zettl Nano Lett., **8**, 3582 (2008).